



HAL
open science

Search for the glueball candidates $f_{O(1500)}$ and $f_{J(1710)}$ in $\gamma\gamma$ collisions

R. Barate, D. Decamp, P. Ghez, C. Goy, J P. Lees, E. Merle, M N. Minard, B. Pietrzyk, R. Alemany, S. Bravo, et al.

► To cite this version:

R. Barate, D. Decamp, P. Ghez, C. Goy, J P. Lees, et al.. Search for the glueball candidates $f_{O(1500)}$ and $f_{J(1710)}$ in $\gamma\gamma$ collisions. Physics Letters B, 2000, 472, pp.189-199. in2p3-00005216

HAL Id: in2p3-00005216

<https://hal.in2p3.fr/in2p3-00005216>

Submitted on 12 May 2000

HAL is a multi-disciplinary open access archive for the deposit and dissemination of scientific research documents, whether they are published or not. The documents may come from teaching and research institutions in France or abroad, or from public or private research centers.

L'archive ouverte pluridisciplinaire **HAL**, est destinée au dépôt et à la diffusion de documents scientifiques de niveau recherche, publiés ou non, émanant des établissements d'enseignement et de recherche français ou étrangers, des laboratoires publics ou privés.

Search for the glueball candidates $f_0(1500)$ and $f_J(1710)$ in $\gamma\gamma$ collisions

The ALEPH Collaboration¹

Abstract

Data taken with the ALEPH detector at LEP1 have been used to search for $\gamma\gamma$ production of the glueball candidates $f_0(1500)$ and $f_J(1710)$ via their decay to $\pi^+\pi^-$. No signal is observed and upper limits to the product of $\gamma\gamma$ width and $\pi^+\pi^-$ branching ratio of the $f_0(1500)$ and the $f_J(1710)$ have been measured to be

$$\Gamma(\gamma\gamma \rightarrow f_0(1500)) \cdot \mathcal{BR}(f_0(1500) \rightarrow \pi^+\pi^-) < 0.31 \text{ keV}$$

and

$$\Gamma(\gamma\gamma \rightarrow f_J(1710)) \cdot \mathcal{BR}(f_J(1710) \rightarrow \pi^+\pi^-) < 0.55 \text{ keV}$$

at 95% confidence level.

Submitted to Phys. Lett. B

¹See next page for the list of authors

The ALEPH Collaboration

- R. Barate, D. Decamp, P. Ghez, C. Goy, J.-P. Lees, E. Merle, M.-N. Minard, B. Pietrzyk
Laboratoire de Physique des Particules (LAPP), IN²P³-CNRS, F-74019 Annecy-le-Vieux Cedex, France
- R. Alemany, S. Bravo, M.P. Casado, M. Chmeissani, J.M. Crespo, E. Fernandez, M. Fernandez-Bosman, Ll. Garrido,¹⁵ E. Graugès, A. Juste, M. Martinez, G. Merino, R. Miquel, Ll.M. Mir, A. Pacheco, I. Riu, H. Ruiz
Institut de Física d'Altes Energies, Universitat Autònoma de Barcelona, E-08193 Bellaterra (Barcelona), Spain⁷
- A. Colaleo, D. Creanza, M. de Palma, G. Iaselli, G. Maggi, M. Maggi, S. Nuzzo, A. Ranieri, G. Raso, F. Ruggieri, G. Selvaggi, L. Silvestris, P. Tempesta, A. Tricomi,³ G. Zito
Dipartimento di Fisica, INFN Sezione di Bari, I-70126 Bari, Italy
- X. Huang, J. Lin, Q. Ouyang, T. Wang, Y. Xie, R. Xu, S. Xue, J. Zhang, L. Zhang, W. Zhao
Institute of High-Energy Physics, Academia Sinica, Beijing, The People's Republic of China⁸
- D. Abbaneo, G. Boix,⁶ O. Buchmüller, M. Cattaneo, F. Cerutti, V. Ciulli, G. Dissertori, H. Drevermann, R.W. Forty, M. Frank, T.C. Greening, A.W. Halley, J.B. Hansen, J. Harvey, P. Janot, B. Jost, I. Lehraus, O. Leroy, P. Mato, A. Minten, A. Moutoussi, F. Ranjard, L. Rolandi, D. Schlatter, M. Schmitt,²⁰ O. Schneider,² P. Spagnolo, W. Tejessy, F. Teubert, E. Tournefier, A.E. Wright
European Laboratory for Particle Physics (CERN), CH-1211 Geneva 23, Switzerland
- Z. Ajaltouni, F. Badaud, G. Chazelle, O. Deschamps, A. Falvard, C. Ferdi, P. Gay, C. Guicheney, P. Henrard, J. Jousset, B. Michel, S. Monteil, J-C. Montret, D. Pallin, P. Perret, F. Podlyski
Laboratoire de Physique Corpusculaire, Université Blaise Pascal, IN²P³-CNRS, Clermont-Ferrand, F-63177 Aubière, France
- J.D. Hansen, J.R. Hansen, P.H. Hansen,¹ B.S. Nilsson, B. Rensch, A. Wäänänen
Niels Bohr Institute, DK-2100 Copenhagen, Denmark⁹
- G. Daskalakis, A. Kyriakis, C. Markou, E. Simopoulou, I. Siotis, A. Vayaki
Nuclear Research Center Demokritos (NRCD), GR-15310 Attiki, Greece
- A. Blondel, G. Bonneaud, J.-C. Brient, A. Rougé, M. Rumpf, M. Swynghedauw, M. Verderi, H. Videau
Laboratoire de Physique Nucléaire et des Hautes Energies, Ecole Polytechnique, IN²P³-CNRS, F-91128 Palaiseau Cedex, France
- E. Focardi, G. Parrini, K. Zachariadou
Dipartimento di Fisica, Università di Firenze, INFN Sezione di Firenze, I-50125 Firenze, Italy
- M. Corden, C. Georgiopoulos
Supercomputer Computations Research Institute, Florida State University, Tallahassee, FL 32306-4052, USA^{13,14}
- A. Antonelli, G. Bencivenni, G. Bologna,⁴ F. Bossi, P. Campana, G. Capon, V. Chiarella, P. Laurelli, G. Mannocchi,^{1,5} F. Murtas, G.P. Murtas, L. Passalacqua, M. Pepe-Altarelli
Laboratori Nazionali dell'INFN (LNF-INFN), I-00044 Frascati, Italy
- L. Curtis, J.G. Lynch, P. Negus, V. O'Shea, C. Raine, P. Teixeira-Dias, A.S. Thompson
Department of Physics and Astronomy, University of Glasgow, Glasgow G12 8QQ, United Kingdom¹⁰
- R. Cavanaugh, S. Dhamotharan, C. Geweniger,¹ P. Hanke, G. Hansper, V. Hepp, E.E. Kluge, A. Putzer, J. Sommer, K. Tittel, S. Werner,¹⁹ M. Wunsch¹⁹
Institut für Hochenergiephysik, Universität Heidelberg, D-69120 Heidelberg, Germany¹⁶

R. Beuselinck, D.M. Binnie, W. Cameron, P.J. Dornan, M. Girone, S. Goodsir, E.B. Martin, N. Marinelli, A. Sciabà, J.K. Sedgbeer, E. Thomson, M.D. Williams

Department of Physics, Imperial College, London SW7 2BZ, United Kingdom¹⁰

V.M. Ghete, P. Girtler, E. Kneringer, D. Kuhn, G. Rudolph

Institut für Experimentalphysik, Universität Innsbruck, A-6020 Innsbruck, Austria¹⁸

C.K. Bowdery, P.G. Buck, A.J. Finch, F. Foster, G. Hughes, R.W.L. Jones, N.A. Robertson, M.I. Williams

Department of Physics, University of Lancaster, Lancaster LA1 4YB, United Kingdom¹⁰

I. Giehl, K. Jakobs, K. Kleinknecht, G. Quast, B. Renk, E. Rohne, H.-G. Sander, H. Wachsmuth, C. Zeitnitz

Institut für Physik, Universität Mainz, D-55099 Mainz, Germany¹⁶

J.J. Aubert, A. Bonissent, J. Carr, P. Coyle, P. Payre, D. Rousseau

Centre de Physique des Particules, Faculté des Sciences de Luminy, IN²P³-CNRS, F-13288 Marseille, France

M. Aleppo, M. Antonelli, F. Ragusa

Dipartimento di Fisica, Università di Milano e INFN Sezione di Milano, I-20133 Milano, Italy

V. Büscher, H. Dietl, G. Ganis, K. Hüttmann, G. Lütjens, C. Mannert, W. Männer, H.-G. Moser, S. Schael, R. Settles, H. Seywerd, H. Stenzel, W. Wiedenmann, G. Wolf

Max-Planck-Institut für Physik, Werner-Heisenberg-Institut, D-80805 München, Germany¹⁶

P. Azzurri, J. Boucrot, O. Callot, S. Chen, A. Cordier, M. Davier, L. Duflot, J.-F. Grivaz, Ph. Heusse, A. Jacholkowska,¹ F. Le Diberder, J. Lefrançois, A.-M. Lutz, M.-H. Schune, J.-J. Veillet, I. Videau,¹ D. Zerwas

Laboratoire de l'Accélérateur Linéaire, Université de Paris-Sud, IN²P³-CNRS, F-91898 Orsay Cedex, France

G. Bagliesi, T. Boccali, C. Bozzi,¹² G. Calderini, R. Dell'Orso, I. Ferrante, L. Foà, A. Giassi, A. Gregorio, F. Ligabue, P.S. Marrocchesi, A. Messineo, F. Palla, G. Rizzo, G. Sanguinetti, G. Sguazzoni, R. Tenchini,¹ A. Venturi, P.G. Verdini

Dipartimento di Fisica dell'Università, INFN Sezione di Pisa, e Scuola Normale Superiore, I-56010 Pisa, Italy

G.A. Blair, G. Cowan, M.G. Green, T. Medcalf, J.A. Strong

Department of Physics, Royal Holloway & Bedford New College, University of London, Surrey TW20 OEX, United Kingdom¹⁰

D.R. Botterill, R.W. Clift, T.R. Edgecock, P.R. Norton, J.C. Thompson, I.R. Tomalin

Particle Physics Dept., Rutherford Appleton Laboratory, Chilton, Didcot, Oxon OX11 0QX, United Kingdom¹⁰

B. Bloch-Devaux, P. Colas, S. Emery, W. Kozanecki, E. Lançon, M.-C. Lemaire, E. Locci, P. Perez, J. Rander, J.-F. Renardy, A. Roussarie, J.-P. Schuller, J. Schwindling, A. Trabelsi,²¹ B. Vallage

CEA, DAPNIA/Service de Physique des Particules, CE-Saclay, F-91191 Gif-sur-Yvette Cedex, France¹⁷

S.N. Black, J.H. Dann, R.P. Johnson, H.Y. Kim, N. Konstantinidis, A.M. Litke, M.A. McNeil, G. Taylor

Institute for Particle Physics, University of California at Santa Cruz, Santa Cruz, CA 95064, USA²²

C.N. Booth, S. Cartwright, F. Combley, M. Lehto, L.F. Thompson

Department of Physics, University of Sheffield, Sheffield S3 7RH, United Kingdom¹⁰

K. Affholderbach, A. Böhrer, S. Brandt, C. Grupen, J. Hess, A. Misiejuk, G. Prange, U. Sieler

Fachbereich Physik, Universität Siegen, D-57068 Siegen, Germany¹⁶

G. Giannini, B. Gobbo

Dipartimento di Fisica, Università di Trieste e INFN Sezione di Trieste, I-34127 Trieste, Italy

J. Rothberg, S. Wasserbaech

Experimental Elementary Particle Physics, University of Washington, WA 98195 Seattle, U.S.A.

S.R. Armstrong, P. Elmer, D.P.S. Ferguson, Y. Gao, S. González, O.J. Hayes, H. Hu, S. Jin, J. Kile, P.A. McNamara III, J. Nielsen, W. Orejudos, Y.B. Pan, Y. Saadi, I.J. Scott, J. Walsh, J.H. von Wimmersperg-Toeller, Sau Lan Wu, X. Wu, G. Zobernig

Department of Physics, University of Wisconsin, Madison, WI 53706, USA¹¹

¹Also at CERN, 1211 Geneva 23, Switzerland.

²Now at Université de Lausanne, 1015 Lausanne, Switzerland.

³Also at Centro Siciliano di Fisica Nucleare e Struttura della Materia, INFN, Sezione di Catania, 95129 Catania, Italy.

⁴Also Istituto di Fisica Generale, Università di Torino, 10125 Torino, Italy.

⁵Also Istituto di Cosmo-Geofisica del C.N.R., Torino, Italy.

⁶Supported by the Commission of the European Communities, contract ERBFMBICT982894.

⁷Supported by CICYT, Spain.

⁸Supported by the National Science Foundation of China.

⁹Supported by the Danish Natural Science Research Council.

¹⁰Supported by the UK Particle Physics and Astronomy Research Council.

¹¹Supported by the US Department of Energy, grant DE-FG0295-ER40896.

¹²Now at INFN Sezione de Ferrara, 44100 Ferrara, Italy.

¹³Supported by the US Department of Energy, contract DE-FG05-92ER40742.

¹⁴Supported by the US Department of Energy, contract DE-FC05-85ER250000.

¹⁵Permanent address: Universitat de Barcelona, 08208 Barcelona, Spain.

¹⁶Supported by the Bundesministerium für Bildung, Wissenschaft, Forschung und Technologie, Germany.

¹⁷Supported by the Direction des Sciences de la Matière, C.E.A.

¹⁸Supported by the Austrian Ministry for Science and Transport.

¹⁹Now at SAP AG, 69185 Walldorf, Germany.

²⁰Now at Harvard University, Cambridge, MA 02138, U.S.A.

²¹Now at Département de Physique, Faculté des Sciences de Tunis, 1060 Le Belvédère, Tunisia.

²²Supported by the US Department of Energy, grant DE-FG03-92ER40689.

1 Introduction

Quantum chromodynamics (QCD) predicts the existence of bound states of gluons, called glueballs. Lattice calculations have predicted the lightest scalar glueball to be a scalar resonance with mass $1600 \pm 150 \text{ MeV}/c^2$ [1, 2] with tensor and pseudoscalar glueballs in the $2000 - 2500 \text{ MeV}/c^2$ region [3].

Experimentally two principal candidates for the scalar glueball have been observed, the $f_0(1500)$ and the $f_J(1710)$ (a review is given in [4]). Both are seen in gluon-rich reactions such as $p\bar{p}$ annihilation, central production and radiative J/ψ decay. The $f_0(1500)$ does not fit naturally in the $q\bar{q}$ spectrum but could be due to a glueball mixed with $q\bar{q}$ states in that mass region [5].

The spin of the $f_J(1710)$ is not yet confirmed, indications for both spin 2 and spin 0 have been reported [4, 6]. If the $f_J(1710)$ is indeed spin 0 it becomes a candidate for the $^3P_0(s\bar{s})$ -like state in the $1600 - 2000 \text{ MeV}/c^2$ region, but also for the lightest scalar glueball [2].

In $\gamma\gamma$ interactions, production of a pure gluon state is suppressed. Measuring the two-photon width $\Gamma_{\gamma\gamma}$ of the $f_0(1500)$ and the $f_J(1710)$, or setting an upper limit on $\Gamma_{\gamma\gamma}$, should indicate whether either is likely to be a pure glueball or has quark content. The CLEO collaboration has recently published a stringent limit on the two-photon width of the $f_J(2220)$ resonance (formerly the $\xi(2220)$) which is a candidate for the tensor glueball [13].

At the LEP e^+e^- collider there is a large cross-section for inelastic two-photon scattering, in which each of the incoming electrons acts as a source of virtual photons. In this analysis, the processes $\gamma\gamma \rightarrow f_0(1500) \rightarrow \pi^+\pi^-$ and $\gamma\gamma \rightarrow f_J(1710) \rightarrow \pi^+\pi^-$ have been studied and upper limits extracted for $\Gamma_{\gamma\gamma} \cdot \mathcal{BR}(\pi^+\pi^-)$ of both resonances.

2 The ALEPH detector

The ALEPH detector and its performance are described in detail elsewhere [7, 8]. Here only a brief description of the detector components relevant for this analysis is given.

The trajectories of charged particles are measured with a silicon vertex detector (VDET), a cylindrical multiwire drift chamber (ITC) and a large time projection chamber (TPC). The three detectors are immersed in a 1.5 T axial magnetic field from the superconducting solenoidal coil and together provide a transverse momentum resolution $\delta p_{\perp}/p_{\perp} = 6 \times 10^{-4} p_{\perp} \oplus 0.005$ (p_{\perp} in GeV/c). The TPC also provides up to 338 measurements of ionisation (dE/dx) used for particle identification.

Between the TPC and the coil, an electromagnetic calorimeter (ECAL) is used to identify electrons and photons and to measure their energy with a relative resolution of $0.18/\sqrt{E} + 0.009$ (E in GeV). The luminosity calorimeters (LCAL and SiCAL) cover the small polar angle region, 24–190 mrad.

Muons are identified by their characteristic penetration pattern in the hadron calorimeter (HCAL), a 1.2 m thick iron yoke instrumented with 23 layers of limited streamer tubes, together with two surrounding layers of muon chambers. In association with the electromagnetic calorimeter, the hadron calorimeter also provides a measurement of the energy of charged and neutral hadrons with a relative resolution of $0.85/\sqrt{E}$ (E in GeV).

The main ALEPH trigger relevant for this analysis, for data taken in 1994 and after, is based on the identification of two track candidates in the ITC, with at least one track pointing to an energy deposit in excess of 200 MeV in the ECAL. The two track candidates are confirmed at the second trigger level using the TPC. For data taken before 1994, the analysis relies on a trigger of two ITC (and TPC) track candidates measured back-to-back within 11° .

3 Monte Carlo samples

Fully simulated Monte Carlo event samples reconstructed with the same program as the data have been used for the design of the event selection, background estimation and extraction of a limit on two-photon widths $\Gamma_{\gamma\gamma}^{f_0(1500)}$ and $\Gamma_{\gamma\gamma}^{f_J(1710)}$. Samples of the signal processes $\gamma\gamma \rightarrow f_0(1500) \rightarrow \pi^+\pi^-$ and $\gamma\gamma \rightarrow f_J(1710) \rightarrow \pi^+\pi^-$ were generated using PHOT02 [9]. Each sample was generated as a Breit-Wigner resonance of appropriate mass, width and spin, with the $f_J(1710)$ here assumed to be spin zero. The experimental resolution of the masses of both resonances is of the order of $10 \text{ MeV}/c^2$, compared to full widths in excess of $100 \text{ MeV}/c^2$.

Expected background processes $\gamma\gamma \rightarrow e^+e^-$, $\gamma\gamma \rightarrow \mu^+\mu^-$, and $\gamma\gamma \rightarrow \tau^+\tau^-$ were also generated using PHOT02, while background from $e^+e^- \rightarrow Z \rightarrow \tau^+\tau^-$ was estimated using KORALZ [10]. Both programs are interfaced to the JETSET [11] package for hadronisation, while KORALZ also includes TAUOLA [12] for correct handling of the τ polarisation.

4 Event selection

This analysis uses 160.9 pb^{-1} of data taken around $\sqrt{s} = 91 \text{ GeV}$ from 1990 to 1995. Candidate events for $\gamma\gamma \rightarrow \pi^+\pi^-$ are selected according to the following criteria:

- the event contains only two good tracks, of equal and opposite charge. Good tracks are defined to have at least four TPC hits, $|\cos\theta| < 0.93$, where θ is the polar angle with respect to beam axis, and a minimum distance to the interaction point of less than 8 cm along the beam axis and 2 cm in the radial direction;
- the total energy summed over all objects reconstructed by the energy flow program is equal to the total energy of the two charged tracks;
- the primary vertex is reconstructed within $\pm 2 \text{ cm}$ of the nominal interaction point along the beam axis;
- the total energy observed in the event is less than 30 GeV and visible mass less than 10 GeV, to exclude Z events;
- the transverse momentum of the final state with respect to the beam axis does not exceed $0.1 \text{ GeV}/c$;
- the absolute value of the cosine of the angle θ^* between the two tracks in their centre-of-mass system and the boost direction is required to be less than 0.9.

These criteria ensure (quasi-)real photon ($Q^2 = 0$) collisions, and also suppress three- or more body decay.

The dominant background to the two-pion signal is the $\gamma\gamma \rightarrow \mu^+\mu^-$ process. At low energies, muons and pions cannot easily be distinguished from each other and the high cross-section for the $\gamma\gamma \rightarrow \mu^+\mu^-$ process leads to a substantial contamination of the $\pi^+\pi^-$ sample.

To reduce background, events containing identified muons [8] are rejected. With a sample of $\gamma\gamma \rightarrow \mu^+\mu^-$ events generated using PHOT02, it was found that the efficiency of rejection is about 100% for events with invariant mass $W > 3 \text{ GeV}/c^2$. Below $W = 3 \text{ GeV}/c^2$, the rejection efficiency is improved by means of simple cuts on the fraction of energy deposited in the ECAL and HCAL, but still the rejection efficiency falls off rapidly, being only $\sim 20\%$ for $W = 1 \text{ GeV}/c^2$. For $W \geq 1 \text{ GeV}/c^2$ the average rejection efficiency for $\gamma\gamma \rightarrow \mu^+\mu^-$ events is 45%.

After muon rejection, the specific ionisation (dE/dx) of each track, measured in the TPC, is required to be within three standard deviations of the expected ionisation for a pion and more than three standard deviations from that of an electron. Separation of pions and kaons by dE/dx is less efficient, but the rate of kaon pair production is low: from a Monte Carlo sample of $f_2'(1525) \rightarrow K^+K^-$, a residual contamination of only $\sim 0.05\%$ was estimated.

Possible background from beam-gas interactions was investigated. Constraining the reconstructed primary vertex position in z removes most of this background. As beam-gas events are uniformly distributed in z , the number of events falling outside the z -vertex cut can be used to estimate the remaining background inside the cut: beam-gas contamination is found to be negligible. Residual backgrounds from the processes $\gamma\gamma \rightarrow \tau^+\tau^-$ and $Z \rightarrow \tau^+\tau^-$ are also negligible.

A sample of 294141 $\pi^+\pi^-$ candidate events is selected.

5 Fitting the mass spectrum

The $\pi^+\pi^-$ invariant mass spectrum obtained is shown in Fig. 1. The step rise of the spectrum around $0.5 \text{ GeV}/c^2$ is an artefact of the trigger efficiency. The clear peak in the spectrum above $1 \text{ GeV}/c^2$ can be identified as the known tensor resonance $f_2(1270)$. No other structure is observed above the $f_2(1270)$ peak.

A fit to the invariant mass spectrum is performed. For the resonances $f_2(1270)$, $f_0(1500)$ and $f_J(1710)$, a Breit-Wigner function of the form

$$\frac{mm_0\Gamma(m)}{(m_0^2 - m^2)^2 + m^2\Gamma^2(m)} \quad (1)$$

is used, where the mass-dependent width $\Gamma(m)$, away from the two-pion threshold, has the form

$$\Gamma(m) = \Gamma_0 \left(\frac{m}{m_0}\right)^{(l+1/2)} \exp\left[\frac{-(m^2 - m_0^2)}{48\beta^2}\right] \quad (2)$$

and $\beta = 0.4 \text{ GeV}/c^2$ [14]. For the $f_2(1270)$ the mass m_0 , total width Γ_0 and overall normalisation are free parameters. For the $f_0(1500)$ and the $f_J(1710)$ the normalisation is a free parameter, while the mass and width are fixed to $1500 \text{ MeV}/c^2$ and $112 \text{ MeV}/c^2$ for the $f_0(1500)$ and $1712 \text{ MeV}/c^2$ and $133 \text{ MeV}/c^2$ for the $f_J(1710)$ [4]. The $f_J(1710)$ is

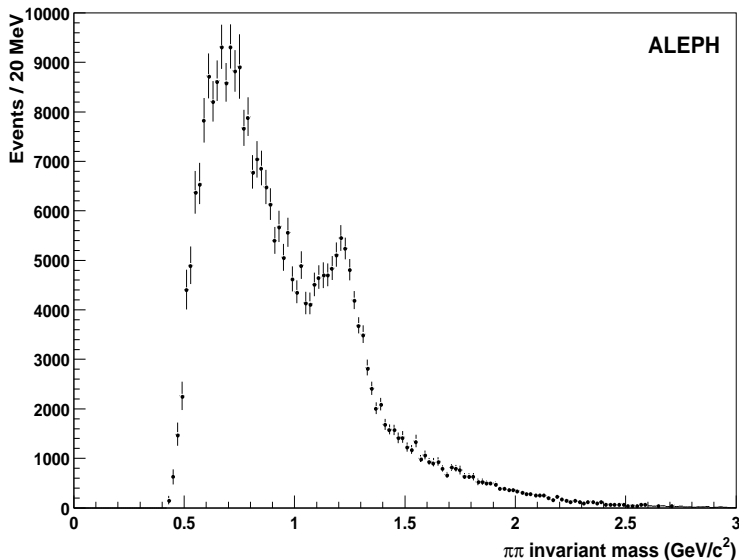


Figure 1: The invariant mass distribution for two-pion final states. The error bars indicate statistical errors only.

considered here as a $J = 0$ state. Although the presence of two objects in the $1700 \text{ MeV}/c^2$ region has been suggested [15], no attempt to resolve two objects is made here.

The background spectrum, due to $\gamma\gamma \rightarrow \mu\mu$ events and the $\pi\pi$ continuum process, is fitted on the data with a 5th order Chebyshev polynomial.

The mass region 0.8 to $2.5 \text{ GeV}/c^2$ is used in the fit (below $0.8 \text{ GeV}/c^2$ the trigger efficiency falls to less than 20%). Four fits are performed, each including a Breit-Wigner for the $f_2(1270)$ and the polynomial background and then including

- (i) no additional resonances,
- (ii) the $f_0(1500)$,
- (iii) the $f_J(1710)$,
- (iv) both the $f_0(1500)$ and the $f_J(1710)$.

The fit to the data is shown in Fig. 2 for case (i): the Breit-Wigner shape for the $f_2(1270)$, the polynomial for background processes and the sum of these are indicated.

The parameters of all fits are summarised in Table 1, including the number of events fitted for the glueball candidate signals. For the fit including the $f_2(1270)$ alone, the χ^2 of 75 for 76 degrees of freedom is already very good. The χ^2 per degree of freedom hardly changes with the addition of glueball signals. The fits including the $f_J(1710)$ were also performed for $J = 2$. The results of these fits were essentially the same as for the $J = 0$ case.

The width of the Breit-Wigner function fitted for the $f_2(1270)$ is in all cases in agreement with the world average value of $185.5^{+3.8}_{-2.7} \text{ MeV}/c^2$ [4]. The fitted mass of $\sim 1214 \text{ MeV}/c^2$ in each case is not consistent with the established value of $1275.0 \pm 1.2 \text{ MeV}/c^2$ [4], however. This has been previously observed by the MARKII and CELLO collaborations [16] and is believed to be caused by interference of the spin 2 resonant amplitude with other components in the background.

Limited knowledge of the trigger efficiency for this topology prevents an investigation of interference effects using the measured angular distribution. The number of events fitted for the $f_0(1500)$ signal is negative, but consistent with zero. Data from the WA76

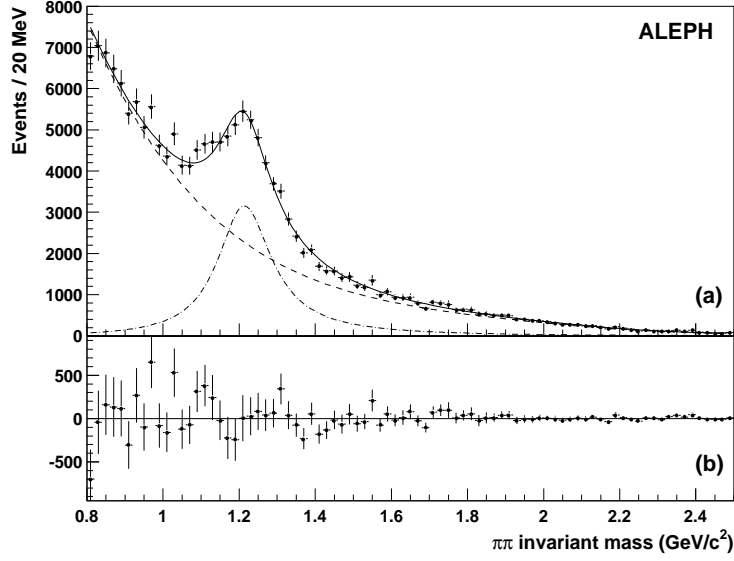


Figure 2: (a) The fit to data with a Breit-Wigner function for the $f_2(1270)$ (dot-dash line), a polynomial for the background (dashed line) and the combination of these functions (solid line); and (b) the data after subtraction of the fitted curve. Error bars indicate statistical errors only.

Table 1: Table of parameters for fits using the Breit-Wigner form of Eqn.1 for resonances.

	(i) Fit for $f_2(1270)$ only
χ^2	74.96
Degrees of freedom	76
Fitted mass of $f_2(1270)$ (MeV/ c^2)	1213.5 ± 3.7
Fitted width of $f_2(1270)$ (MeV/ c^2)	178.3 ± 12.8
	(ii) Fit for $f_2(1270) + f_0(1500)$
χ^2	73.33
Degrees of freedom	75
Fitted mass of $f_2(1270)$ (MeV/ c^2)	1214.1 ± 3.8
Fitted width of $f_2(1270)$ (MeV/ c^2)	173.9 ± 13.8
No. of $f_0(1500)$ signal events	-808.3 ± 602.6
	(iii) Fit for $f_2(1270) + f_J(1710)$
χ^2	74.02
Degrees of freedom	75
Fitted mass of $f_2(1270)$ (MeV/ c^2)	1213.9 ± 3.9
Fitted width of $f_2(1270)$ (MeV/ c^2)	180.2 ± 15.9
No. of $f_J(1710)$ signal events	468.3 ± 476.6
	(iv) Fit for $f_2(1270) + f_0(1500) + f_J(1710)$
χ^2	73.21
Degrees of freedom	74
Fitted mass of $f_2(1270)$ (MeV/ c^2)	1214.2 ± 3.8
Fitted width of $f_2(1270)$ (MeV/ c^2)	175.5 ± 14.2
No. of $f_0(1500)$ signal events	-671.0 ± 690.0
No. of $f_J(1710)$ signal events	198.6 ± 541.9

and WA102 collaborations [17] and recent calculations [18] suggest interference effects in this region can cause the $f_0(1500)$ to appear as a dip in the spectrum. However, here limits are set assuming no interference.

The CELLO collaboration has reported possible structure in the $\pi^+\pi^-$ invariant mass spectrum around $1.1 \text{ GeV}/c^2$ [19]. If the fit of case (i) is repeated but excluding a region around $1.1 \text{ GeV}/c^2$, a clear excess of data over the fitted curve extrapolated through that region can be seen (Fig. 3a). The excess can be described by the introduction of another spin 0 resonance of apparent mass $\sim 1.1 \text{ GeV}/c^2$ and total width $\sim 250 \text{ MeV}/c^2$ (Fig. 3b).

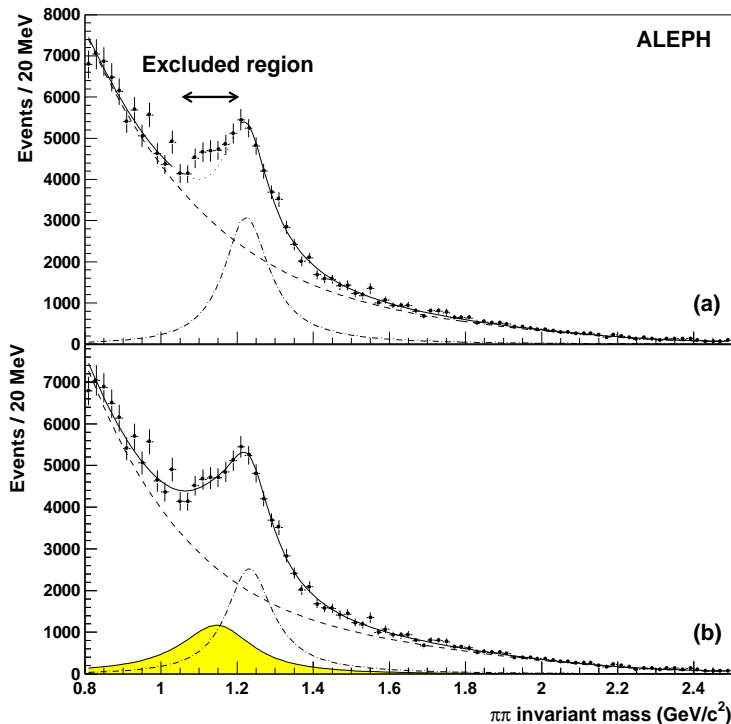


Figure 3: The fit to data is shown with a Breit-Wigner function for the $f_2(1270)$ (dot-dash line), a polynomial for the background (dashed line) and the sum of these functions (solid line), where (a) the region around $1.1 \text{ GeV}/c^2$ is excluded from the fit – the extrapolation of the fit through the excluded region is indicated by the dotted line; and (b) a second Breit-Wigner function has been introduced around $1.1 \text{ GeV}/c^2$ (shaded region) and is included in the total fit (solid line). All error bars indicate statistical errors only.

6 $\Gamma_{\gamma\gamma} \cdot \mathcal{BR}(\pi^+\pi^-)$ for $f_0(1500)$ and $f_J(1710)$

The fitted numbers of signal events from the processes $\gamma\gamma \rightarrow f_0(1500) \rightarrow \pi^+\pi^-$ and $\gamma\gamma \rightarrow f_J(1710) \rightarrow \pi^+\pi^-$ are used to calculate upper limits on $\Gamma_{\gamma\gamma} \cdot \mathcal{BR}(\pi^+\pi^-)$ for both resonances.

The trigger efficiency is calculated as a function of invariant mass by comparing rates of independent triggers for $\pi^+\pi^-$ selected data. In the $1500 \text{ MeV}/c^2$ mass region the average trigger efficiency is $(66 \pm 7)\%$, while for the $1700 \text{ MeV}/c^2$ mass region it is $(77 \pm 7)\%$.

The acceptance and selection efficiency for $\gamma\gamma \rightarrow f_0(1500) \rightarrow \pi^+\pi^-$ and for $\gamma\gamma \rightarrow f_J(1710) \rightarrow \pi^+\pi^-$ are determined from Monte Carlo to be $(17.5 \pm 0.4)\%$ and $(16.3 \pm 0.4)\%$, where the quoted errors include the systematic error due to the simulation of the detector (checked by varying the resolution on measured quantities used in the event selection) and the error due to Monte Carlo statistics.

The product branching ratio, $\Gamma_{\gamma\gamma} \cdot \mathcal{BR}(\pi^+\pi^-)$, of each resonance is calculated directly from the fitted number of signal events in each of the cases (ii)–(iv). The fitted value of $\Gamma_{\gamma\gamma} \cdot \mathcal{BR}(\pi^+\pi^-)$ (which may be negative) and its error are used to define the mean and width of a Gaussian distribution: the area under the Gaussian is integrated above zero to obtain the 95% C.L. limit on $\Gamma_{\gamma\gamma} \cdot \mathcal{BR}(\pi^+\pi^-)$.

The upper limits on the product branching ratios at 95% C.L. are, for the individual fits, $\Gamma_{\gamma\gamma} \cdot \mathcal{BR}(\pi^+\pi^-) < 0.25$ keV and $\Gamma_{\gamma\gamma} \cdot \mathcal{BR}(\pi^+\pi^-) < 0.59$ keV for the $f_0(1500)$ and $f_J(1710)$ respectively, and for the combined fit are $\Gamma_{\gamma\gamma} \cdot \mathcal{BR}(\pi^+\pi^-) < 0.31$ keV and $\Gamma_{\gamma\gamma} \cdot \mathcal{BR}(\pi^+\pi^-) < 0.55$ keV for the $f_0(1500)$ and $f_J(1710)$ respectively. If an additional spin 0 resonance with a fixed mass of 1.1 GeV/ c^2 (as discussed in section 5) is included in the combined fit, the limit on the product branching ratio for the $f_0(1500)$ worsens by $\sim 30\%$ and for the $f_J(1710)$ tightens by $\sim 10\%$.

The analysis was repeated using the same Breit-Wigner form for the resonances but with an alternative expression for the mass-dependent width that has been used in some previous experimental resonance studies [20]:

$$\Gamma(m) = \Gamma_0 \cdot \frac{2 \cdot \left(\frac{m^2 - 4m_\pi^2}{m_0^2 - 4m_\pi^2}\right)^{l+\frac{1}{2}}}{1 + \frac{m^2 - 4m_\pi^2}{m_0^2 - 4m_\pi^2}}. \quad (3)$$

The fitted parameters and numbers of signal events are given in Table 2. The χ^2 per degree of freedom for each of these fits is considerably worse than for the original fits.

The upper limit on $\Gamma_{\gamma\gamma} \cdot \mathcal{BR}(\pi^+\pi^-)$ for the case when only the $f_0(1500)$ is included is 0.33 keV, and for the $f_J(1710)$ only is 0.84 keV. For the case including both resonances, the upper limits are 0.28 keV and 0.69 keV for the $f_0(1500)$ and the $f_J(1710)$ respectively. These limits are consistent with the original results.

7 Stickiness

From limits on $\Gamma_{\gamma\gamma}$ the *stickiness* [21] of each resonance can be calculated, by comparison of the two photon width with the particle's width for production in the glue-rich environment of radiative J/ψ decay. The ratio is normalised such that the $q\bar{q}$ resonance $f_2(1270)$ has stickiness equal to 1. Then for a glueball a higher value of stickiness is expected.

Stickiness for a 0^{++} resonance X is defined as

$$S_X(0^{++}) = \mathcal{N} \frac{m_X}{k_{J/\psi \rightarrow \gamma X}} \frac{\Gamma(J/\psi \rightarrow \gamma X)}{\Gamma(X \rightarrow \gamma\gamma)}$$

where m_X is the mass of the resonance; $k_{J/\psi \rightarrow \gamma X} = (m_{J/\psi}^2 - m_X^2)/2m_{J/\psi}$ is the energy of the photon from the radiative J/ψ decay, measured in the J/ψ rest frame; $\Gamma(J/\psi \rightarrow \gamma X)$ is the width for production of the resonance in radiative J/ψ decay; and \mathcal{N} is the normalisation factor. The branching ratio for $f_0(1500) \rightarrow \pi^+\pi^-$ is taken as 0.30 ± 0.07 , while the branching ratio for $f_J(1710) \rightarrow \pi^+\pi^-$ is $0.026_{-0.016}^{+0.001}$ [4], giving, from the fit for

Table 2: Table of parameters for fits using an alternative expression for the mass-dependent width of all resonances.

	(i) Fit for $f_2(1270)$ only
χ^2	108.36
Degrees of freedom	76
Fitted mass of $f_2(1270)$ (MeV/ c^2)	1216.2 ± 18.5
Fitted width of $f_2(1270)$ (MeV/ c^2)	221.3 ± 18.2
	(ii) Fit for $f_2(1270) + f_0(1500)$
χ^2	88.48
Degrees of freedom	75
No. of $f_0(1500)$ signal events	-1549.4 ± 901.9
	(iii) Fit for $f_2(1270) + f_J(1710)$
χ^2	89.81
Degrees of freedom	75
No. of $f_J(1710)$ signal events	1019.8 ± 475.6
	(iv) Fit for $f_2(1270) + f_0(1500) + f_J(1710)$
χ^2	87.51
Degrees of freedom	74
No. of $f_0(1500)$ signal events	-1242.8 ± 741.1
No. of $f_J(1710)$ signal events	485.2 ± 576.0

both resonances, $\Gamma(f_0(1500) \rightarrow \gamma\gamma) = 1.08$ keV and $\Gamma(f_J(1710) \rightarrow \gamma\gamma) = 21.25$ keV. The lower limits on stickiness are then 1.4 and 0.3 for the $f_0(1500)$ and the $f_J(1710)$ respectively.

8 Conclusion

Production of the glueball candidates $f_0(1500)$ and $f_J(1710)$ in $\gamma\gamma$ collisions at LEP1 has been studied via decay to $\pi^+\pi^-$. No signal from either resonance is seen, and the upper limits on the product of two-photon width and $\pi^+\pi^-$ branching ratio have been calculated as $\Gamma_{\gamma\gamma} \cdot \mathcal{BR}(\pi^+\pi^-) < 0.31$ keV for the $f_0(1500)$ and $\Gamma_{\gamma\gamma} \cdot \mathcal{BR}(\pi^+\pi^-) < 0.55$ keV for the $f_J(1710)$, both at 95% C.L., from a simultaneous fit for both resonances.

Acknowledgements

We wish to thank our colleagues from the accelerator divisions for the successful operation of LEP. We are indebted to the engineers and technicians at CERN and our home institutes for their contribution to the good performance of ALEPH. Those of us from non-member countries thank CERN for its hospitality.

References

- [1] UKQCD Collaboration, *A Comprehensive Lattice Study of $SU(3)$ Glueballs*, Phys. Lett. **B309** (1993) 378.
- [2] J. Sexton, A. Vaccarino and D. Weingarten, Phys. Rev. Lett **75** (1995) 4563.
- [3] A. Szczepaniak, E.S. Swanson, C.-R. Ji and S.R. Cotanch, Phys. Rev. Lett **76** (1996) 2011.
- [4] Particle Data Group, Eur. Phys. J. **C3** (1998) 1.
- [5] For example, C. Amsler and F.E. Close, Phys. Rev. **D53** (1996) 295.
- [6] WA102 Collaboration, *A partial wave analysis of the centrally produced K^+K^- and $K_s^0K_s^0$ systems in pp interactions at 450 GeV/c*, Phys. Lett. **B453** (1999) 305.
- [7] ALEPH Collaboration, *ALEPH: A Detector for Electron-Positron Annihilations at LEP*, Nucl. Instrum. Meth **A294** (1990) 121.
- [8] ALEPH Collaboration, *Performance of the ALEPH Detector at LEP*, Nucl. Instrum. Meth **A360** (1995) 481.
- [9] ALEPH Collaboration, *An Experimental study of $\gamma\gamma \rightarrow$ hadrons at LEP*, Phys. Lett. **B313** (1993) 509.
- [10] S. Jadach, B.F.L. Ward and Z. Wąs, Comp. Phys. Comm. **79** (1994) 503.
- [11] T. Sjöstrand, Computer Phys. Commun. **82** (1994) 74.
- [12] R. Decker, S. Jadach and Z. Wąs, Comp. Phys. Comm. **76** (1993) 361.
- [13] CLEO Collaboration, *Further Search for the Two-Photon Production of the Glueball Candidate $f_J(2220)$* , Phys. Rev. Lett. **81** (1998) 3328.
- [14] A. Donnachie, private communication.
- [15] BES Collaboration, *Structure Analysis of the $f_J(1710)$ in the Radiative Decay $J/\psi \rightarrow \gamma K^+ K^-$* , Phys. Rev. Lett **77** (1996) 3959.
- [16] J. Boyer *et al.* (MARK II Collaboration), *Two-Photon Production of Pion Pairs*, Phys. Rev. **D42** (1990) 1350; J.E. Olsson, in Proc. of 5th Intern. Colloquium on Photon Photon Collisions (1983) Aachen.
- [17] WA76 Collaboration, *Study of the Centrally Produced $\pi\pi$ and $K\bar{K}$ Systems at 85 and 300 GeV/c*, Z. Phys. **C51** (1991) 351; WA102 Collaboration, *A Partial Wave Analysis of the Centrally Produced $\pi^+\pi^-$ System in pp Interactions at 450 GeV/c*, Phys. Lett. **B453** (1999) 324.
- [18] A.V. Anisovich, V.V. Anisovich, Phys. Lett. **B467** (1999) 289.
- [19] CELLO Collaboration, *An Experimental Study of the Process $\gamma\gamma \rightarrow \pi^+\pi^-$* , Z. Phys. **C56** (1992) 381.

- [20] OMEGA Photon Collaboration, *Comparison of Photon and Hadron Induced Production of ρ^0 Mesons in the Energy Range 65 to 175 GeV*, Z. Phys. **C53** (1992) 581.
- [21] M. Chanowitz, in Proc. of the VI Intern. Workshop on Photon-Photon Collisions (1984) Lake Tahoe.